ASIAN JOURNAL OF CIVIL ENGINEERING (BHRC) VOL. 16, NO. 2 (2015)
PAGES 161-181

IN-PLANE RIGIDITY OF LATERALLY LOADED COMPOSITE FLOOR SYSTEMS, A FINITE ELEMENT APPROACH

S. M. Zahrai* and L. Sarkissian
Center of Excellence for Engineering and Management of Infrastructures, School of Civil Engineering, The University of Tehran, Tehran, Iran

Received: 20 February 2014; **Accepted:** 6 October 2014

ABSTRACT

The influence of the in-plane flexibility of composite floor systems on the seismic response of the structures may become significant, particularly when considerable floor slab cracking and yielding are expected. As in recent years the use of composite floor systems is increasing, in this study the lateral in-plane behavior of composite floor diaphragms in steel structures is investigated through numerical simulations. The structures considered in the study were two models of the prototype buildings, where the elastic and inelastic responses of the diaphragms under lateral load are analyzed using 3-D finite element models and FEM linear and nonlinear structural analysis. It was found that under the seismic load specified in the code, the criterion of diaphragm rigidity is too small, so the composite floor systems can be assumed as rigid body, however under lateral loads with higher amplitudes, by developing the cracks in the concrete slabs, nonlinear behavior and stiffness degradation of the diaphragms might occur. The results showed that for both single story structures the ultimate strength of the diaphragms was very high about 20 to 33 times of the seismic load specified in Iran's seismic code, however the ultimate strength of the second model, where the joists direction was perpendicular to the lateral load direction, was considerable showing a reduction about 50~60% compared to the ultimate strength of the first model, where the joists direction was parallel to the lateral load direction. The comparisons between the numerical and previously obtained experimental results showed that FEM overestimates the diaphragm response in terms of stiffness and deformability; however conservatively estimates the diaphragms strength.

Keywords: Composite floor system; numerical simulation; nonlinear analysis; diaphragm; seismic load; crack pattern; ultimate strength; in-plane stiffness.

*E-mail address of the corresponding author: mzahrai@ut.ac.ir (S.M. Zahrai)

1. INTRODUCTION

The contribution of the floor systems in transferring the lateral loads (seismic actions, wind pressures, etc.) to the vertical structural elements and subsequently to the foundation of the building structures is well known and indisputable. The floor systems in building structures, are usually designed to carry the gravity loads, however they should be also designed to resist the lateral forces and be able to transfer them to the resisting systems by a diaphragm action. If the floor elements act together in resisting the horizontal action to have the same deflection showing high in-plane lateral stiffness,the floor performance is known as rigid diaphragm behavior. In current design practice of building structures, the floor subassembly, according to the specifications of many building codes is usually considered as a rigid diaphragm. Even this assumption is often used to reduce the degrees of freedom of the structure and simplifies seismic response analysis of many types of buildings, however for some classes of structural systems, the effect of diaphragm deformability cannot be disregarded, especially in the case of rectangular buildings with large aspect ratios where considerable inelastic floor slab behavior is expected [1]. Since the diaphragm behavior is one of the most important factors in the seismic response of the structures, researchers have conducted studies on this subject, but the studies do not have a long precedent and they have been mostly performed in the last two decades.

The influence of floor plan shape on the earthquake response of buildings were studied and to quantify the impact of floor plan shape, two dimensionless parameters MCE and CVE, related to maximum potential energy stored at the critical element divided by the mean for that floor, and the coefficient of variation of the potential energy stored in the resisting elements all over the plan respectively, were defined, as for the ideal rectangular building with rigid diaphragms MCE=1 and CVE=0 [1]. An extended numerical parametric study was carried out to study the diaphragm behavior of RC floor systems (slabs and beams). The results show that the influence of aspect ratio on the criterion of the diaphragms rigidity (Δ_d / Δ_s) is considerable, although there is no clear correlation between these two structural characteristics [2].

The behavior of a post-frame building diaphragm was investigated through an extensive test program on a full scale actual post-frame building. The building was tested during the different phases of construction to evaluate the contribution of components of the building system in the lateral load resisting action. The behavior of the two roof halves acted like a unite diaphragm, because of the continuity provided by the roof framing system, but after installing the mid shear wall the two roof walls acted as two separate diaphragms [3]. The studies on the low rise steel buildings with metal roof deck have shown that the lateral period is influenced by the diaphragm in-plane flexibility and the forces in the resistant elements can be amplified due to dynamics of the flexible diaphragm, also the shaking table results have indicated that the diaphragm in-plane deformations are twice of the values obtained from static analysis [4].

The investigations on the PBFB floors (Prestressed Beams and Filler Blocks) have shown that a 4 cm thick slab for these floors assures the validity of "rigid diaphragm" hypothesis and the horizontal resistance capacity of the floors with cast-in-place concrete over the entire area were twice of the floors without that and with transversal reinforcement, also the failure modes of the specimens were very different, depending on material of filler blocks and

presence or absence of cast in place over concrete [5]. The seismic behavior of wood diaphragms in unreinforced masonry buildings has been studied through the tests on three test specimens, using different rehabilitation methods. The results indicate that FEMA 273 tended to over-predict the stiffness and significantly under-predict yield displacement and ultimate deformation levels, while FEMA 356 tended to under-predict stiffness and over-predict yield displacement [6].

Barron and Hueste in 2004 evaluated the impact of in-plane diaphragm deformation on the structural response of typical RC rectangular buildings using a performance-based approach. Three and five-story RC buildings with end shear walls and two aspect ratios were developed and designed according to current code procedures assuming rigid diaphragm behavior. They found that the use of a flexible diaphragm model had the largest impact on the three-story, 3:1 aspect ratio building and that the various analysis procedures in FEMA273 gave different adequacy assessments for this case study building [7].

Paquette and Bruneau in 2006 studied the response of wood diaphragm and its interaction with shear walls through tests on a full-scale one-story unreinforced brick masonry specimen having the wood diaphragm subjected to earthquake excitations using pseudo-dynamic testing. The FEMA 306 procedure proved the most accurate for evaluation purposes while others missed one or more points of behavior. Although not tested to its ultimate capacity, the diaphragm deflections experimentally observed, closely matched those predicted using the FEMA 356 and ABK models [8].

Floor diaphragm behavior is a combination of both in-plane and out-of-plane loadings. However, in some previous research, the diaphragm behavior of a floor slab was represented by its behavior under in-plane forces only. With this assumption, analysis of the floor diaphragm was simplified to the two dimensional plane stress problem. For low-rise buildings, the lateral stiffness of the structure is usually higher than high-rise buildings, and then the study of diaphragm behavior and the calculation of interstory drift in these structures are more important as investigated by Lee et al. in 2007 [9, 10].

Khalili Jahromi et al. in 2008 experimentally investigated the diaphragm rigidity of composite floors in a half-scale single-story sample building. The seismic lateral load was simulated by quasi-static reversal cyclic loading and two models were subjected to the quasi-static cyclic lateral loads up to failure. The results showed that the second diaphragm model where joists were perpendicular to the direction of lateral loading has higher lateral in-plane stiffness. There was no significant stiffness degradation until 85% of the ultimate load, but the first diaphragm has lower stiffness and the stiffness degradation started at a load of 48% of the ultimate load [11].

Sadashiva et al. in 2012 carried out a series of elastic and inelastic time history analyses of symmetric structures with different deformation types, configurations and heights to quantify these effects. They found out that displacements of single story elastic structures are greatly affected by diaphragm flexibility. Analyses of these structures were cross-verified by a closed-form mechanics-based formulation developed to describe the response and also proposed simple relationships to allow designers to conservatively estimate the increase in peak in-plane displacement resulting from diaphragm flexibility [12].

Hadianfard and Sedaghat in 2013 investigated the nonlinear responses of braced steel buildings with flexible concrete block-joist floor diaphragms under both static lateral load and dynamic ground motion, and compared them with the responses of structures with the

assumption of rigid diaphragms. They showed that span ratio is an important parameter in the flexibility of floor diaphragms, and for the cases with this ratio greater than three, the variation of results between the two assumptions of flexible and rigid diaphragms may not be ignored [13].

Abeysinghe et al. in 2013 studied the dynamic performance of an innovative Hybrid Composite Floor Plate System (HCFPS) using experimental testing and Finite Element modeling. Parametric studies were conducted using the validated FE models to investigate the dynamic response of the HCFPS and to identify characteristics that influence acceleration response under human induced vibration in service. They showed that HCFPS as a light-weight floor system can be well used in residential and office buildings without exceeding the perceptible thresholds due to human induced vibrations [14]. Da Silvaa et al. in 2014 utilized three dynamic loading models based on a real steel–concrete composite floor spanning 40 m by 40 m, to simulate human rhythmic activities such as jumping and aerobics. The structural system consisted of a typical composite floor of a commercial building. They found that human rhythmic activities could induce the composite floors to reach unacceptable vibration levels leading to a violation of the current human comfort criteria [15].

The diaphragm behavior of different types of floor systems usually differs substantially and depends on the details of the floor system, as in some cases the diaphragms behavior may be unknown. Thus the experiments could be useful to better understand the diaphragms behavior, as many of the analytical studies on this subject have been verified with experiments. As the use of composite floors is increasing, due to their low weight and economic benefits, in this paper the behavior of composite floor systems (CFS) (steel beams with upper concrete slab) in typical steel structures under lateral load with the influence of the gravity load is investigated. The objective of this research is to analyze the composite diaphragms under lateral and gravity loads and to determine the in-plane characteristics of the diaphragm such as the deformability, stiffness, ultimate strength, yield point and crack pattern. Also the analytical results are verified with those obtained from previous experiments. This paper describes the FEM models, linear and nonlinear analyses and presents related main findings.

2. ANALYTICAL MODELS OF THE FLOOR DIAPHRAGMS WITH LINEAR BEHAVIOR

2.1 Design and description of prototype buildings

The structures considered in this study are 3-D single-story typical steel buildings consisting of composite floor and X bracings, common in many countries. The 10.8m x 7.2m x 3m prototype buildings considered in the study are illustrated in Fig. 1. The girders and floor joists are *I* shapes supported on box columns braced by X bracings having box sections. The overall geometry of the structures presented in Fig. 1 is the same and the main difference is the direction of the floor joists.

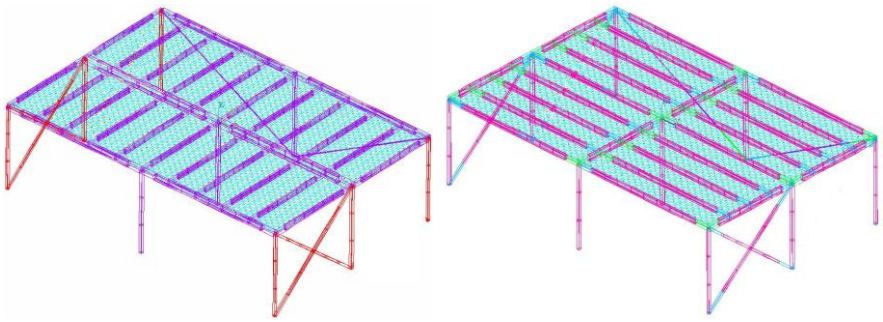

(a) (b)

Figure 1. The steel buildings prototype: (a) The floor joists parallel to the lateral load. (b) The floor joists perpendicular to the lateral load.

The gravity dead and live loads applied on the floor were determined with the specifications of the loading code of Iran [16]. The dead load is calculated using the floor detail presented in Fig. 2. Since the composite floor systems are more common in administrative buildings, the live load is considered 200 kg/m^2 [16]. The composite floors were designed with the AISC code specifications and composite structures design handbook [17, 18]. Thickness of the floor slab was obtained as 8cm and the spacing between the floor joists in the structures shown in Fig. 1, were set to 108cm and 90cm respectively.

The seismic design of the structure was performed according to the seismic code of Iran [19], where the specified seismic lateral load for the structure, V, is given by:

$$V = CW, C = \frac{ABI}{R} \tag{1}$$

Where C is the seismic shear force coefficient, A is zonal acceleration, B is the seismic response factor, I is the importance factor, R is the force modification factor and W is the seismic weight of the structure.

For these administrative building structures in Tehran we have:

A=0.35, B=2.5, R=6, I =1

So we have C=0.146 and the total seismic load calculated for both of the structures, obtained from Eq. (1) is 54.1 kN.

2.2 Linear analysis

The linear analysis of the structures was performed using SAP2000 computer program. For each structure two finite element models were developed, in the first models the floors were modeled by SHELL element having four nodes in each element to consider in-plane flexibility of the diaphragm. The beams, columns and bracings were modeled by FRAME element and the connection between these elements was modeled by the coincident nodes. The scaled structures with flexible diaphragm were analyzed under lateral load specified in the seismic code [19], with the influence of gravity load. The FEM model and deformed shape of the structure with flexible diaphragm is presented in Fig. 2(a) and (b). Due to flexibility of the diaphragm the displacement of midpoint of the diaphragm is more than the side points as shown in Fig. 2(b). In the second models rigid diaphragm hypothesis was used

and the floors were modeled by rigid diaphragms. Fig. 2(c) and (d) shows the FEM model and deformed shape of the structure with rigid diaphragm. In this model the displacements of all points of the diaphragm are the same as shown in Fig. 2(d).

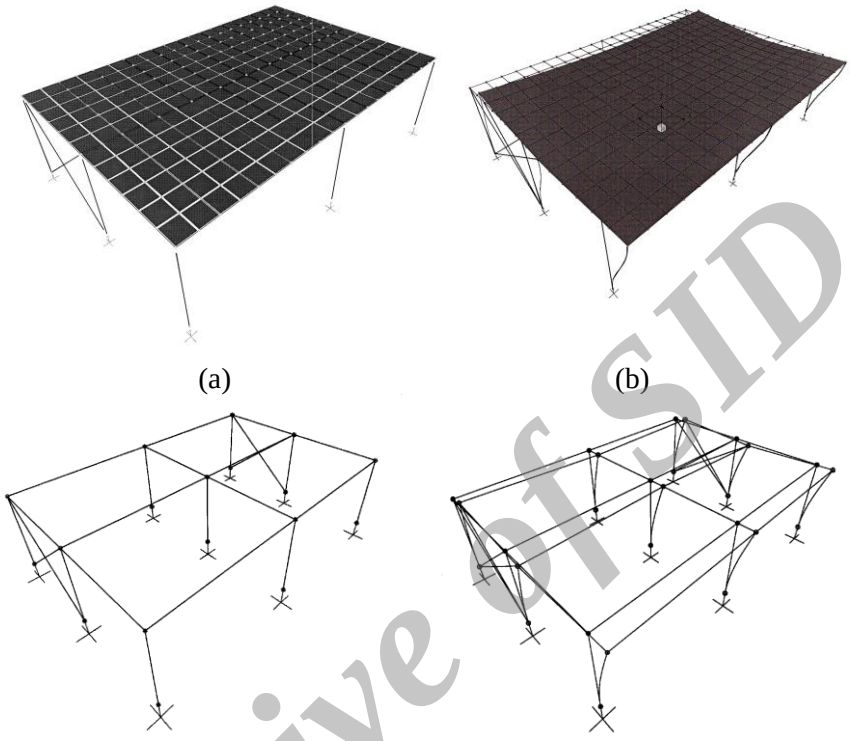

Figure 2. (a) Meshing of the FE Model with Flexible Diaphragm. (b) Deformed Shape. (c) Model of Structure with Rigid Diaphragm. (d) Deformed Shape

2.3 Testing sequence and setup

In order to study the behavior of the composite diaphragms under the lateral load and to compare with the results obtained from FEM linear analysis, the scaled models of the prototype structures presented in Fig. 1 were constructed and tested [11,20, 21]. The compressive strength of the concrete (f_c') was obtained as 19.52 MPa and Young modulus of the concrete was about 20.8 GPa. Also Young modulus and yielding stress of the steel used in bracing members were obtained as 2.09×10^6 kg/cm² and 3900 kg/cm² respectively. The dimensions and plan of the specimens are presented in Fig. 3.

Prior to lateral loading test, gravity load was applied to the structure, including dead and live load and a load related to scaling and simulation requirements given by:

$$Q^{tot} = Q^{DL} + Q^{LL} + Q^{\rho} = 122 + 150 + 100 = 372 \text{ kg/m}^2 \quad (2)$$

In order to have uniform lateral loading, the structures were rotated about the edge axis, because if one side of structure is lifted up or the structure is rotated about the other side

axis, the force tangent to the floor, will act as the seismic lateral shear force.

The tangent component of the gravity force is given by:

$$V=W\sin\alpha \tag{3}$$

Where α=The rotation angle and W=Total weight of the structure.

As in many code the seismic shear force is defined by a weight multiplier (e.g. C factor in eq.(1), from equations (1) and (2) the seismic force coefficient is given by:

$$C=\sin\alpha \tag{4}$$

As mentioned before for this structure C was equal to 0.146, therefore the rotation angel of the structure was about α=8.4˚.

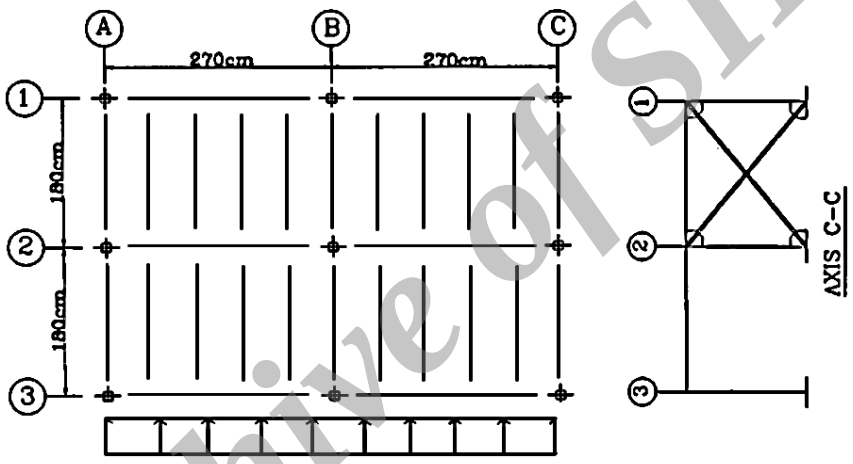

Figure 3. Dimensions, plan and Loading of One of the Specimens

2.4 Results of linear analysis

The results of analysis of the FEM models for both structures and also the results of the rotating tests are presented in Table 1. In this table, RD1 and RD2 are the FE models with rigid diaphragm and FD1 and FD2 are the FE models with flexible diaphragm. Also E1 and E2 are the specimens tested under lateral and gravity loads.

The results show that both of the composite floor diaphragms were rather rigid under the lateral load specified in the seismic code. The differences between the calculated tensile and compressive bracing forces were obtained using Table 1 where for the first specimen were about 17% and 1% respectively, while in the second specimen were 3% and 10.5%.

The net displacement of the diaphragm is the relative displacement of the mid frame to the side frames, which is given by:

$$\Delta_d=\Delta_m-\Delta_s \tag{6}$$

Table 1: Results obtained from three models for the structures

Bracing force(kg)		$\frac{\Delta_d}{\Delta_s}$	Diaph. net disp. (mm)	Story drift (mm)	Diaph. mid disp. (mm)	Lateral load (kg)	Model	
Tensile	Compressive							
429.5	433.1	–	0	0.30498	0.30498	1380	RD1	Sample1-Joists parallel to the lateral load
433.3	426.4	0.07	0.2089	0.29835	0.31924	1380	FD1	
519	429	0.082	0.026	0.319	0.345	1380	E1	
429.5	433.1	–	0	0.30498	0.30498	1380	RD2	Sample2-Joists perpendicular to the lateral load
432.8	426.8	0.068	0.02046	0.29869	0.31915	1380	FD2	
440.8	483.1	0.063	0.020	0.32	0.34	1380	E2	

Where Δ_d is the diaphragm displacement, Δ_m is the displacement of the mid frame and Δ_s is the displacement of the side frames or the story drift. The proportion of $\frac{\Delta_d}{\Delta_s}$ is a criterion to evaluate diaphragms rigidity in some building codes, for example with respect to the specification of Iran's seismic code[19], if $\frac{\Delta_d}{\Delta_s} \leq 0.5$, the diaphragm can be assumed rigid. Since in these structures proportion of $\frac{\Delta_d}{\Delta_s}$ was small (0.063 to 0.083), these composite floors under lateral load behave as rigid diaphragms. One of the effective parameters in the diaphragm behavior of floor systems is aspect ratio of the floor plan, so that for high plan aspect ratios, in-plane flexibility of the diaphragms increases significantly, but there is no clear relation between aspect ratio and $\frac{\Delta_d}{\Delta_s}$ [3, 19]. Therefore in these structures with low aspect ratio (L/D=1.5), the behavior of floor system as a rigid diaphragm, is somehow expectable.

3. ANALYTICAL MODELS FOR THE FLOOR DIAPHRAGMS WITH NONLINEAR BEHAVIOR

3.1 Description of prototype buildings

In some cases floor diaphragm may undergo lateral loads more than the seismic lateral load of a single story building specified in the building codes. For example, the seismic lateral force on a floor diaphragm in lower stories of a multistory building is much more than the seismic lateral load of a single story building with a similar plan. So in the second part of the study, the nonlinear behavior of diaphragms of composite floor systems is studied. In order to ascertain nonlinear behavior of composite diaphragms and study the nonlinear characteristics of diaphragms (such as in-plane deformations, stiffness, ultimate strength, etc.) the stiffness of lateral load resisting system of the structures were increased by

doubling the number of X bracings. It was to give priority to the failure of diaphragms compared to the failure of structures. Structures considered in this part of study and meshing of the FEM models are presented in Fig. 4, where the only difference between these structures and those studied in the first part of the study is the number of bracings. Connections of the columns to the foundation are rigid, while the connection of beams and braces to the columns are hinge.

3.2 Theoretical nonlinear analysis

The seismic load was simulated by lateral cyclic load applied at the roof level distributed on the floor thickness and the pattern of the amplitudes of lateral cyclic load was the same as the previously conducted experiments. The nonlinear analysis of the structures was performed using ANSYS [22]. The elements used in modeling the structures are described as follows.

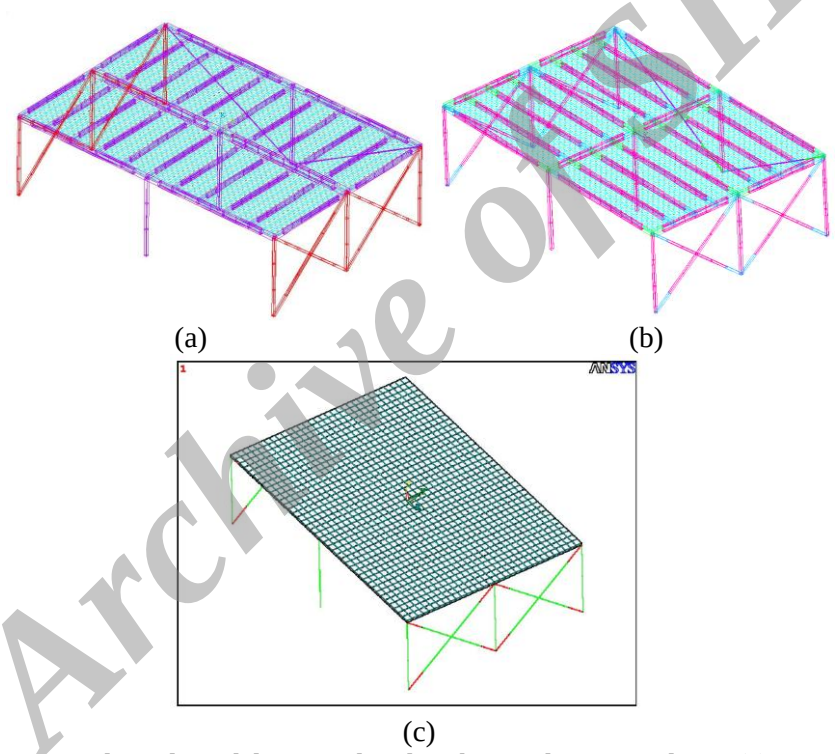

Figure 4. FEM Analytical Models Considered in the Nonlinear Analysis. (a) First Model. (b) Second Model.(c) Meshing of the FEM Models

3.3 Used elements

-SOLID65: SOLID65, capable of cracking in tension and crushing in compression, is used for the three-dimensional modeling of solids with or without reinforcing bars. In concrete applications, for example, the solid capability of the element may be used to model the concrete, while the rebar capability is available for modeling reinforcement behavior. The most important aspect of this element is the treatment of nonlinear properties. The concrete is capable of cracking in three orthogonal directions, crushing, plastic deformation, and

creep. The rebars are capable of tension and compression, but not shear. They are also capable of plastic deformation and creep.

In this study the concrete of composite floor slab is modeled by SOLID65 element and the temperature reinforcement is considered by the volume ratio. The connectivity between the concrete and the steel beams is modeled by common joints within a distance same as the spacing of the shear keys.

-BEAM24: BEAM24 is a uniaxial element of arbitrary cross-section (open or single-celled closed section) with tension-compression, bending and St.Venant torsional capabilities. The element has plastic, creep, and swelling capabilities in the axial direction as well as a user-defined cross section. The element has a stress stiffening, large deflection and shear deflection capabilities. The cross section is defined by a continuous series of rectangular segments in the element y-z plane [22]. In this study BEAM24 element were used to mesh the steel elements of the structural steelwork, such as girders, joists of the composite floors, columns and bracings.

-BEAM44: BEAM44 is a uniaxial element with tension, compression, torsion and bending capabilities. This element allows a different unsymmetrical geometry at each end and permits the end nodes to be offset from the centroidal axis of the beam. Stress stiffening and large deflection capabilities are also included. The application of BEAM24 and BEAM44 elements in developing the FEM model are presented in Fig. 5.

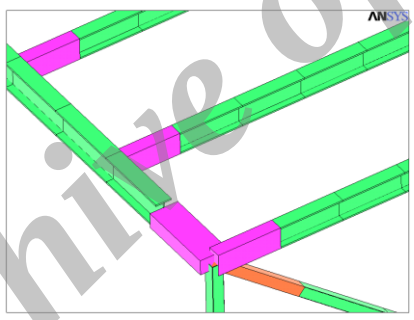

Figure 5. Application of the beam elements in modeling the structures

Since in this element the properties of each end of beam (such as stiffness) may differ, in this study BEAM44 element were used to develop hinge connections of beams and bracings to the columns, so that all steel elements were meshed by BEAM24 element, except the end elements of the beams and braces which were meshed by BEAM44 element, then by releasing the moment of the node located at the connections, hinge connections were created.

3.4 Loading

3.4.1 Gravity load

The gravity load includes dead and live loads and a load related to scaling and simulation requirements (Fig.6). Because as the scale factor is 0.5 the materials used in the scaled structure must be twice of the prototype ones, so to cover the lack of weight, Q_{ρ} a load equal to the weight of concrete slab is considered in total gravity load. The total gravity load applied on the diaphragms is given by:

$$Q_{tot} = Q_{DL} + Q_{LL} + Q_{\rho} = 372 \text{ kg/m}^2 = 3650 \text{ Pa} \quad (2)$$

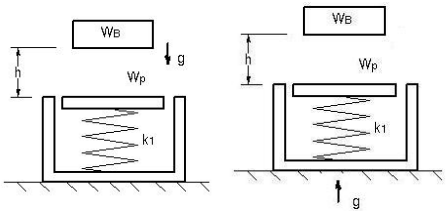

(a) (b)

Figure 6. Applying the structures weight in the software: (a) downward acceleration of the structure.(b) upward acceleration of the base

The total gravity load was applied on SOLID65 element as uniform pressure of 3650 Pa with *Load key=6*. Also the weight of structural elements was included using base acceleration of g=9.8 m/s² upward which is equivalent to acceleration of structural elements downward as shown in Fig. 6 [22].

3.4.2 Lateral load

The lateral load was applied as uniform compressive pressure on the elements located at the edge of the floor slab. Since lateral cyclic load was applied in reverse directions, in the southern edge elements *Load key=2* and in the northern edge elements *Load key=4* were used. Amplitudes of lateral cyclic load in each cycle (which are the same as the previously conducted tests) for both structures are shown in Fig. 7.

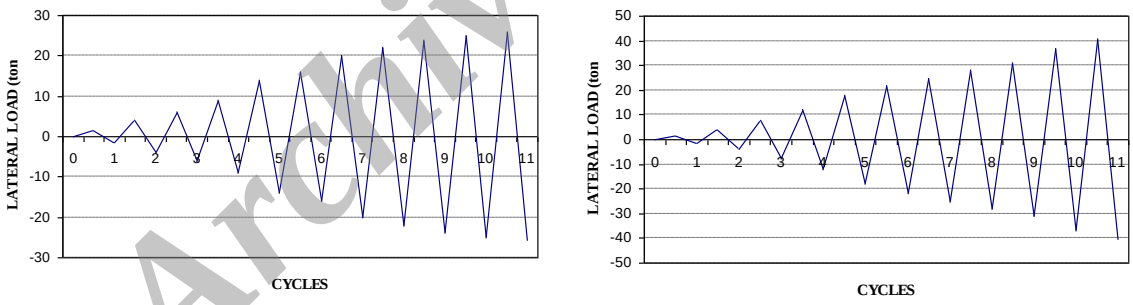

(a) (b)

Figure 7. Amplitudes of Lateral Load. (a) First model. (b) Second model

3.5 Results of nonlinear analysis

3.5.1 Ultimate strength

After loading and unloading in each cycle, the lateral loads of the next cycle were applied with larger amplitude as shown in Fig. 8. The composite diaphragms concrete failed when the solutions of nonlinear analysis were not converging, because despite the time steps were too small and decreased automatically, and also the number of iterations were too large, after a large number of iterations the nonlinear analysis were diverged. The criterion of concrete failure is the criterion of William and Warnke, which represents a surface of failure, using the properties of the concrete, such as uniaxial tensile and compressive stresses and the

coefficients of shear transfer in open and close cracks. The end points of the graphs shown in Fig. 8 relates to the divergence of solutions. According to Fig. 8 the ultimate strength of the diaphragms are 27 tons and 40.8 ton, respectively showing 50% greater ultimate strength for the second diaphragm.

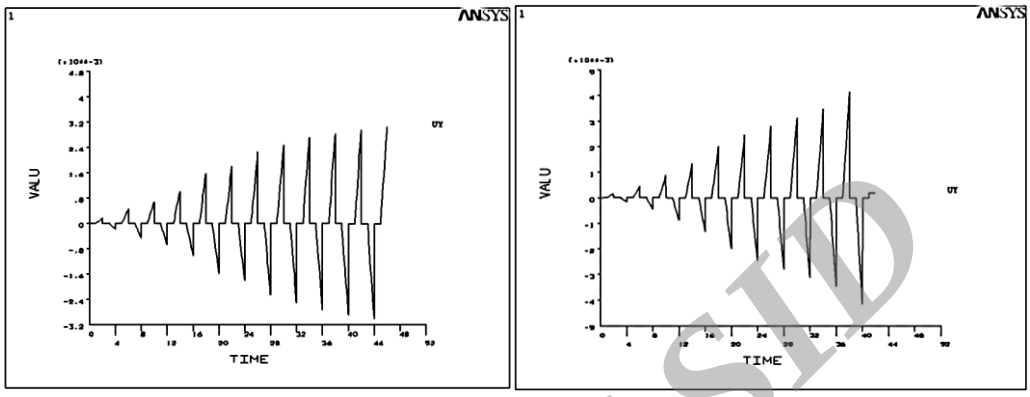

(a) (b)

Figure 8. Solutions of Nonlinear Analysis. (a) First model. (b) Second model

3.5.2 Crack pattern

In both diaphragms some cracks developed under the gravity load which were the same in both models, however cracking under the gravity load were nominal and the main cracks developed under the lateral load. In the first model the first cracks appeared when the lateral load was about 6 tons, then by increasing the lateral load, most of the cracks developed parallel to the joists or the direction of lateral load, but under the loads about the ultimate strength (26 tons), a few cracks developed near the braced frames, which inclined about 45º to the joists. In the second model the first cracks appeared when the lateral load was about 31 tons, then by increasing the lateral load, most of the cracks developed near the braced frames, which inclined about 45º to the joists. Crack patterns of the diaphragms of two models are illustrated in Fig. 9.

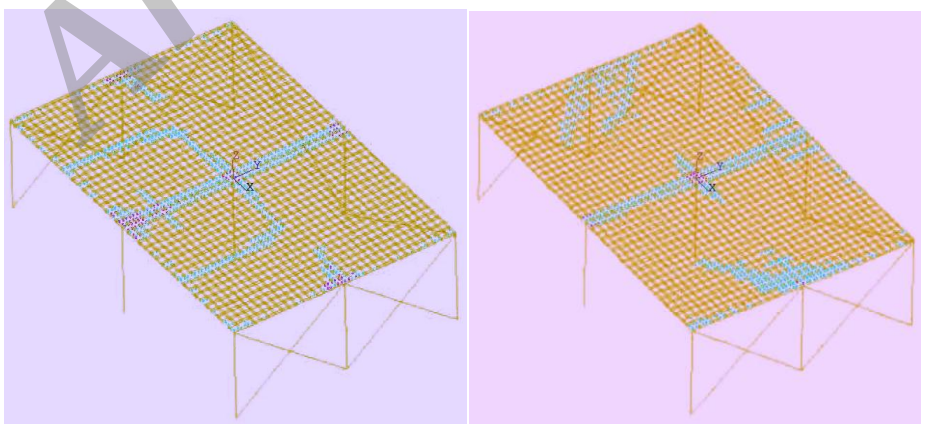

(a) (b)

Figure 9. Crack Patterns of Concrete Slabs of the Diaphragms. (a) First model. (b) Second model

Performance of diaphragms is generally controlled by a combination of shear and flexural actions. In this study, performance of the composite diaphragms can be perceived from the crack patterns of the diaphragms, so that if the diaphragms are considered as beams on the braced frames as their support, in the first model the crack pattern indicates that the flexural action is dominate, but in the second model the crack pattern shows that the shear action is dominant.

3.6 Diaphragm deformation and stiffness

Deformed shapes of the diaphragms were extracted using a path through axis 2-2 (Fig. 4). For example, deformed shape of the diaphragm of the first model under lateral load of 6 tons is illustrated in Fig. 10. The horizontal axis is calibrated as diaphragm width, which is 5.4 m, and the vertical axis presents displacement of all points of the diaphragm. Net displacement of the diaphragm can be found from deformed shapes of diaphragm (such as Fig. 10), which is difference of mid and side frames of the diaphragm.

The analytically obtained load-displacement curves of the diaphragms are shown in Fig. 11. The horizontal axis is the net displacement of the diaphragms and the vertical axis is total lateral load applied on the diaphragm.

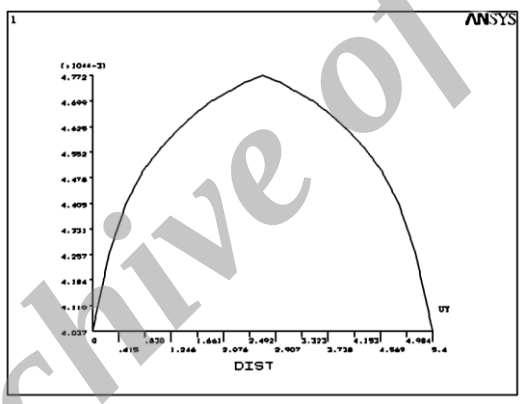

Figure 10. Deformed shape of the first diaphragm

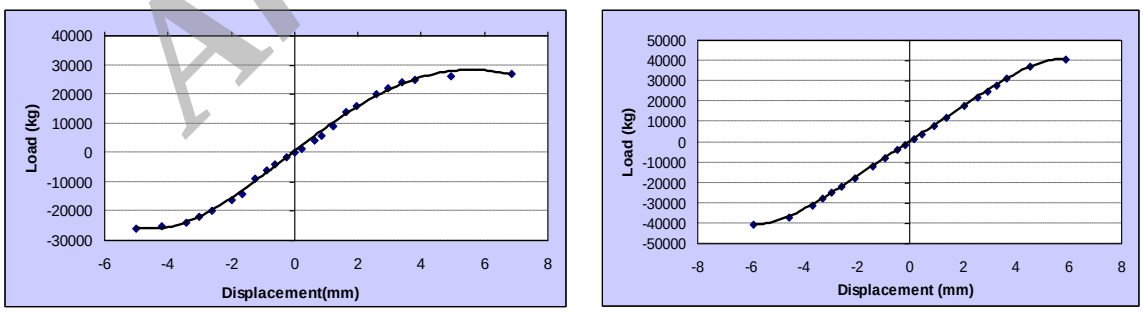

(a) (b)

Figure 11. Load-displacement curves of the diaphragms.(a)First model.(b)Second model

In order to compare in-plane flexibility of the diaphragms, the displacement of two diaphragms versus lateral load is traced in one coordinate system (Fig. 12(a)). As shown in

Fig. 12(a) the displacement of the diaphragms under lateral loads less than 20 tons is almost the same, but under lateral loads more than 20 tons the displacement of the first diaphragm compared to the second one increases significantly. For instance, under ultimate load of the first diaphragm, the displacement of the first diaphragm is about 2.2 times of the second one. The comparison was made in the joint region, since the ultimate strength of the diaphragms was not the same.

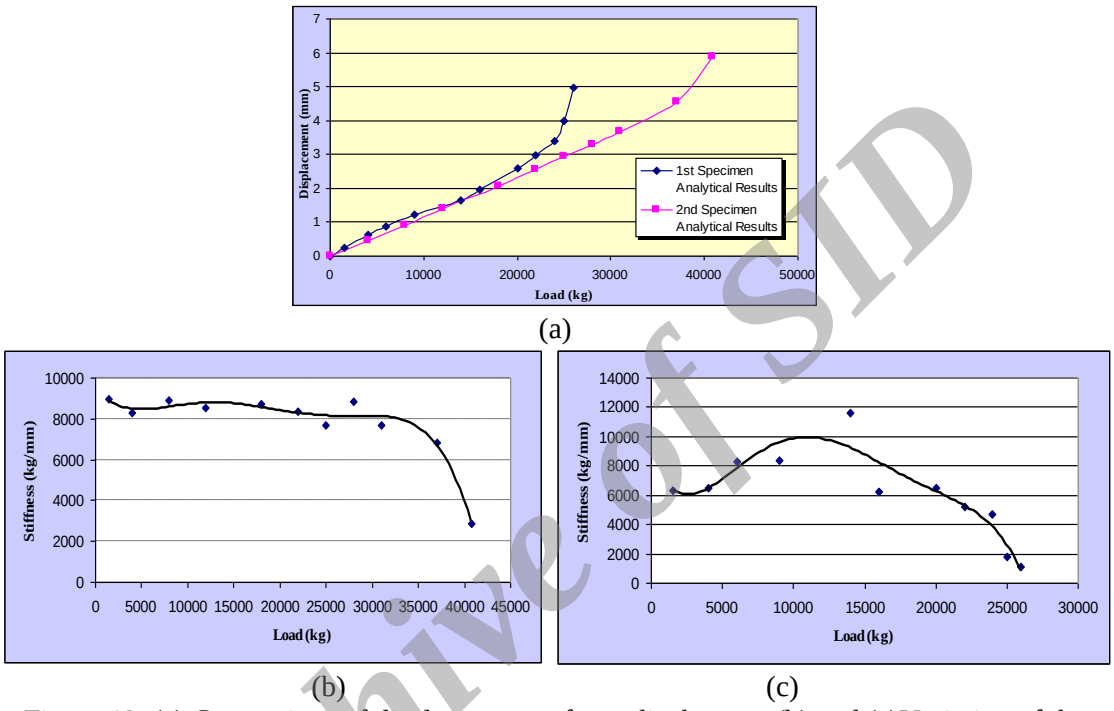

Figure 12. (a) Comparison of displacements of two diaphragms.(b) and (c)Variation of the diaphragms stiffness of First and Second model

One of the most important characteristics of the diaphragms which affect their behavior is their in-plane lateral stiffness. As the stiffness is the load required for unit displacement in a specific point, slope of the load-displacement curves (shown in Fig.12) represents the in-plane stiffness of the diaphragms. Variation of stiffness of two diaphragms versus lateral load is presented in Fig. 12(b) and (c). As shown, in the first model the diaphragm stiffness is rather constant until lateral load reaches 18 tons (about 60% of the ultimate strength), then decreases about 70% until failure. However in the second model the diaphragm stiffness is constant until 34 tons (about 85% of the ultimate strength), then decreases about 50% until failure.

3.7 Stress contours of diaphragms

Since the structures have low plan aspect ratios, the distribution of shear stress in the diaphragms is more important. The contours of shear stress (S_{XY}) in the diaphragms are presented in Fig. 13. Due to the symmetry of the models, the absolute values of shear stress in two sides of the axis of symmetry are the same, but have different signs. As shown in Fig.

14, in both diaphragms the maximum shearing stress is observed near the braced frames. Maximum of the shearing stress for the first diaphragm is about 2.04 MPa ($0.452\sqrt{f'c}$), and for the second diaphragm is about 2.730 MPa ($0.618\sqrt{f'c}$), showing an increase about 36% comparing to the first one.

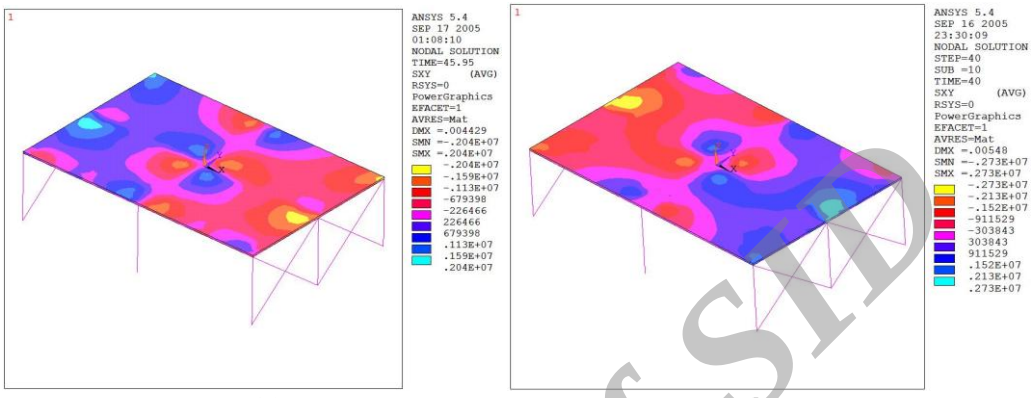

(a) (b)

Figure 13.Contours of Shear Stress in the Diaphragms. (a) First Model. (b) Second Model

4. LATERAL CYCLIC LOADING TEST RESULTS

4.1 Ultimate strength

By increasing the amplitude of lateral load, the failure occurred in the diaphragms of both structures. The diaphragm of the first specimen failed when the lateral load was 29 tons, while the steel structural elements remained elastic, but diaphragm of the second specimen failed when the lateral load was 47 tons, while under ultimate load of the diaphragm, one of the compressive bracings buckled simultaneously. The ultimate strengths of both diaphragms are in good agreement with the results obtained from numerical analysis presented in section 3. The ultimate strengths of the diaphragms, obtained from nonlinear FEM analysis were 27 tons and 40.8 tons respectively, which show errors about 7% and 13% compared to the values obtained from the tests [20].

4.2 Crack pattern

The crack pattern of concrete beams is generally governed by the action of the beam (shear action or flexural action). Since the composite diaphragms can be considered as beams supported by side braced frames, their crack pattern is similar to the crack pattern of concrete beams. In the first diaphragm where the flexural action is dominant, most cracks appeared parallel to the lateral loading direction or the joists direction as shown in Fig. 14(a), however under loads near the ultimate load a few cracks developed which inclined about 45º to the joists. In the second diaphragm the shear action is more dominant and most cracks inclined about 45º to the joists as shown in Fig. 14(b) [20].

(a) (b)

Figure 14. Cracked Shape of Concrete Slab of the Composite Diaphragms after Failure. (a) First specimen. (b) Second Specimen

4.3 Diaphragm deformation and stiffness

The displacements of several points on the diaphragms were measured using sensors through the width of the diaphragms. The experimentally obtained deformed shapes of the diaphragms during the lateral loading test are illustrated in Fig. 15. The horizontal axis of these curves shows the diaphragm width with three frames of the structures, and the vertical axis is the deflection of the points located in the horizontal axis. The curves indicate that the responses are rather smooth and the deflection curves are symmetric. The parabolic shape observed suggests that in addition to the shear deformations of the diaphragm, the flexural deformations are considerable. However the second diaphragm exhibits very high flexural stiffness.

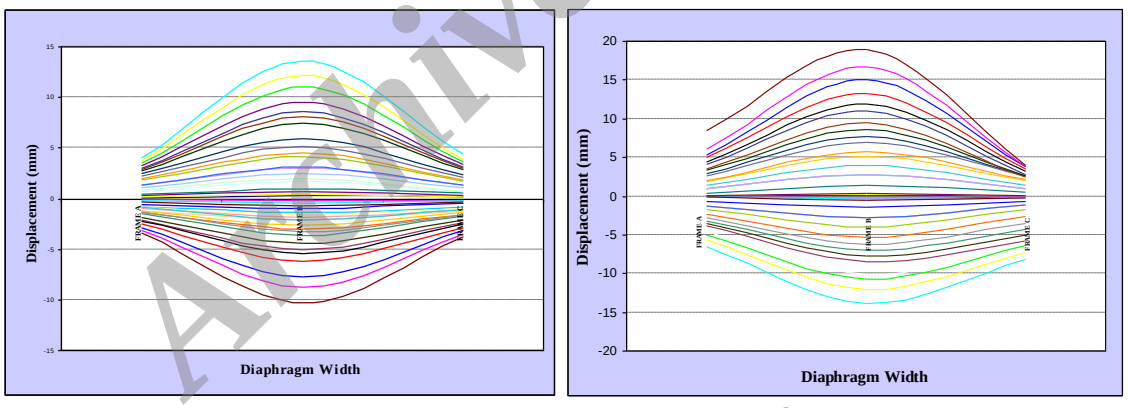

(a) (b)

Figure 15. Deformed shape of the diaphragms. (a) First specimen (b) Second specimen

The hysteretic response of the diaphragms were obtained by the hysteretic response of the braced side frames (A-A and C-C) and the mid frame (B-B), using Eq. (6). As there was no significant stiffness degradation, so the cyclic loading tests were based upon force-control method up to failure.

The envelope curves of hysteretic response of the diaphragms are presented in Fig. 16(a). As there are usually some hidden eccentricities in experimental work, in some cases the displacements of two different sides differ slightly. So the mean values of displacements in

two inverse loading directions (push and pull) were used in envelop curves of Fig. 16(b).

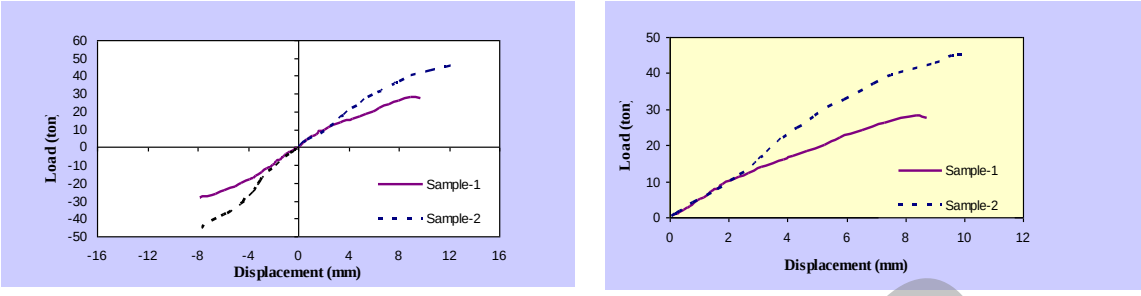

(a) (b)

Figure 16. Envelope of hysteresis curves of the diaphragms. (a) Envelope of cyclic curves for two loading direction (b) Envelope of cyclic curves using average displacement

As shown in Fig. 16(a), for the first diaphragm the ultimate strength was 29 tons and the stiffness was constant until the lateral load was 14 tons, but after developing the cracks, decreased about 50% of the initial stiffness. For the second diaphragm the ultimate strength was 47 tons and the force-displacement curve was linear in a large region and the diaphragm stiffness was approximately constant until the lateral load was about 35 tons, but after that, by developing the first cracks, the diaphragm stiffness decreases about 30 percent of the initial stiffness. The results show that in the second structure which the direction of the floor joists was perpendicular to the direction of the lateral load, the diaphragm has higher in-plane stiffness and ultimate strength compared to the first structure which the direction of the floor joists was parallel to the direction of the lateral load. For example it was observed that the ultimate strength of the second diaphragm was higher than the first one by a factor of 1.63, and the major stiffness degradation of the diaphragms started when the lateral load was 48% and 85% of their ultimate load, respectively. These observations indicate that the second diaphragm generally shows a better performance under lateral loads compared to the second one.

In order to compare the flexibility of the diaphragms, the criterion of diaphragms rigidity (proportion of diaphragm net displacement to the story drift) during the lateral loading test is calculated for both diaphragms. Fig. 17 shows the variation of the criterion of diaphragms rigidity (Δ_d / Δ_s) versus the lateral load applied on the structures.

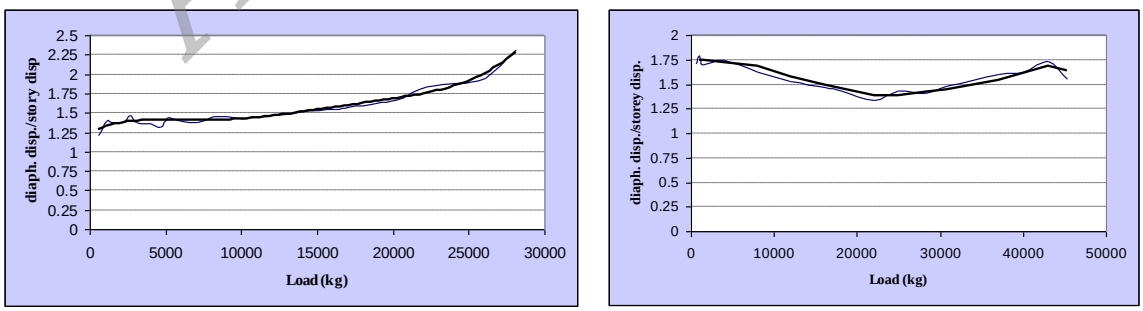

(a) (b)

Figure 17. Variation of the Criterion of Diaphragm Rigidity. (a) First specimen (b) Second Specimen

As shown in Fig. 17(a) for the first specimen the criterion is about 1.5 at first, but by increasing the lateral load the criterion increases significantly and for lateral loads about the ultimate load reaches 2.4. However for the second specimen the criterion during the lateral loading test is about 1.5 and remains almost constant. The graphs shown in Fig. 17 indicate that the diaphragm of the second specimen first exhibits lower in-plane flexibility and represents better performance under lateral load, comparing to the first one which exhibits higher in-plane flexibility.

5. RESULT ANALYSIS

The results of quasi-static cyclic reverse lateral loading test are here compared with those obtained from nonlinear structural analysis by ANSYS. The ultimate strengths of the diaphragms, obtained from nonlinear FEM analysis were 27 tons and 40.8 tons respectively, while the ultimate strengths obtained from the tests were 29 tons and 47 tons, showing errors about 7% and 13%. The difference between the results can be described as follows; ANSYS computer program can predict failure of the concrete using the criterion of William and Warnke [22], which represents a surface of failure, by means of properties of the concrete. However after failure of the concrete, some other structural elements, such as the columns, braces and the joists, and also the interlocking of the temperature reinforcement with the concrete and the joists, resist the lateral load until overall failure of the structure; so the ultimate strength of both diaphragms obtained from the tests are slightly higher than the analytical ones.

As shown in Fig. 14 the crack pattern of both diaphragms, observed in the test, are in good agreement with the crack pattern of concrete obtained from numerical analysis using ANSYS illustrated in Fig. 9. As shown in Fig. 9 and 14, in the diaphragm of the first specimen most cracks are parallel to the direction of lateral load, but in the diaphragm of the second specimen most cracks are inclined about 45º to the joists, showing that the test results confirm the results of FEM nonlinear analysis.

According to the results obtained in section 3, it is obvious that for both diaphragms the finite element method generally underpredicts the diaphragms displacements under lateral load and overpredicts the diaphragms stiffness compared to the ones obtained from tests. In order to compare the displacements obtained from the analytical and experimental research, for both diaphragms the displacements are graphed versus lateral load in one coordinate system as shown in Fig. 18. The difference between the results of two methods can be described as follows; in FEM analysis of diaphragms, size of the elements affect the displacement values of the response, and if the discretisation mesh is not fine enough the stresses of the lateral resisting elements may be determined with a good approximation, but the displacements may be determined with some errors. In modeling of the structures, with respect to the hardware abilities, the diaphragms were meshed by 11.25 cm x 13.5 cm elements as shown in Fig. 5(c), so by using finer elements in meshing of the diaphragms, the analytical displacements of the diaphragms may be closer to the experimental ones. Also concrete is not a homogeneous material and has rather complicated behavior, so modeling the concrete by simplified material models may result in inaccurate results in the nonlinear analysis of concrete elements.

The results analysis show that if two individual diaphragms are designed under gravity load with the same conditions, the diaphragm with joists perpendicular to the lateral load, exhibits a better performance under lateral loads, so it is recommended that in a building with low plan aspect ratio, composite floor systems are so constructed that the direction of the joists in the vicinity of braced frames or shear walls, is perpendicular to the direction that the main lateral load resisting elements act, or the joists are set in a staggered manner all over the plan. If a building has a high plan aspect ratio, directing the joists in the long direction would lead to better performance of the composite diaphragm, however in some cases directing the joists to be perpendicular to the lateral load would be with some penalties, because if the joists are in the long direction of the diaphragm, they are less efficient under gravity load and it would be more costly.

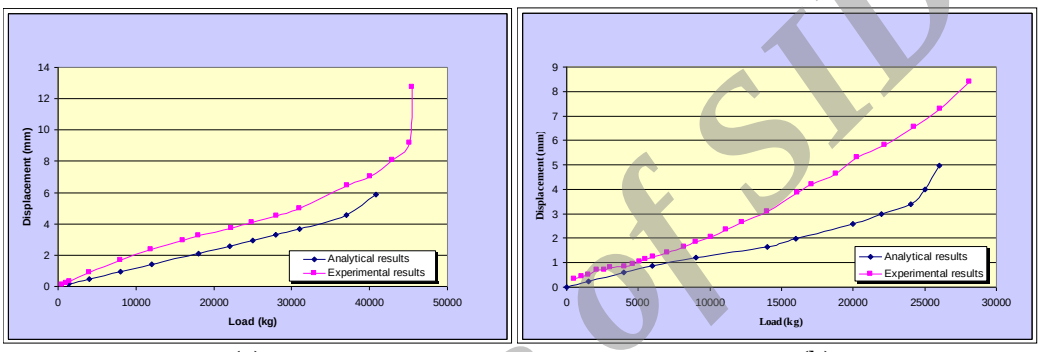

(a) (b)

Figure 18. Comparison of the displacements of the diaphragms obtained from two methods. (a) first specimen (b) second specimen

6. CONCLUSIONS

In this paper the behavior of composite diaphragms was studied in two parts, in the first part the diaphragms were subjected to the lateral seismic load specified in the seismic code and distribution of the lateral load among the resistant elements was studied using FEM analysis with rigid diaphragm and flexible diaphragm hypothesizes and verified with the results of the tests on the half scale specimens. The results of the first part of the study show that:

1-Under the seismic load specified in Iranian seismic code, the criterion of diaphragm rigidity (Δ_d / Δ_s) is too low and the diaphragms can be assumed rigid.

2- The forces of bracings calculated from the methods have errors less than 17%, which indicates that using the rigid floor diaphragm model provides adequate results for the stresses of the laterally resisting vertical structural elements and the story drift.

In the second part of the study, the behavior of the composite diaphragms under lateral loading, in the cases that the diaphragms are subjected to lateral loads with large amplitudes, were studied. The models considered in the first part after increasing the stiffness of the side braced frames, were subjected to the quasi-static cyclic lateral load up to failure. The results of the second part of the study show that:

1-The second diaphragm has higher lateral in-plane stiffness and there was no significant

stiffness degradation until 85% of the ultimate load, but the first diaphragm had lower stiffness and the stiffness degradation started at a load of 48% of the ultimate load.

2-The ultimate strength of the second diaphragm was considerable showing a reduction about 50~60% compared to that of the first diaphragm.

3-For both single story structures the ultimate strength of the diaphragms was very high about 20 and 33 times of the seismic load specified in Iranian seismic code, respectively.

4- The comparisons between the numerical and experimental results previously obtained by the authors showed that FEM overestimates the diaphragm response in terms of stiffness and deformability; however FEM conservatively estimates the diaphragms strength.

5-It seems that one of the most important parameters in the diaphragm behavior of the composite floor systems is the relative direction of the joists to the lateral load and it is recommended that the composite floor systems are so constructed that the joists direction is perpendicular to the direction toward which the main lateral load resisting elements act.

Acknowledgments: The financial support provided by Building and Housing Research Center of Iran (BHRC) who founded this research, is appreciated. The authors alsowish to express their appreciation to Mr. K. Khalili Jahromi and technical staff of the structural engineering laboratory of BHRC, for their useful collaboration in this project.

REFERENCES

1. Lopez OA, Anichiarico W, Genatios C. The influence of floor plan shape on the earthquake response of buildings, *Proceedings 10th European Conference on Earthquake Engineering*, Rotterdam, 1995.
2. Doudoumis N, Athanatopoulou AM. Modeling the floor diaphragm action of multi-story buildings with 2-D finite element models, *Proceedings Conference on Seismic Design Practice into the Next Century*, Rotterdam, 1998.
3. Gebremedhin KG, Price J. Tests of post-frame building diaphragm, *Journal of Structural Engineering, ASCE*, No. 10, **125**(1999) 1170-8.
4. Tremblay R, Berair T, Filiatrault A. Experimental behavior of low-rise steel buildings with flexible roof diaphragms, *12WCEE*, Auckland, New Zealand, 2000.
5. Damian A, Kovacs LA, Bia CT, Octavian G, Maniu H,Dico CS, Tokes A. Diaphragm behavior of the floor with pre-stressed beam and filler blocks, *12WCEE*, Auckland, New Zealand, 2000.
6. Peralta DF, Bracci JM, Hueste MBD. Seismic behavior of wood diaphragms in pre-1950 unreinforced masonry buildings, *Journal of Structural Engineering, ASCE*, No. 10, **130**(2004) 1487-96.
7. Barron JM, Hueste MB. Diaphragm effects in rectangular reinforced concrete, *ACI Structural Journal*, No. 5, **101**(2004) 615-24.
8. Paquette J, Bruneau M. Pseudo-dynamic testing of unreinforced masonry building with flexible diaphragm and comparison with existing procedures, *Journal of Construction and Building Materials*, **20**(2006) 220-8.
9. Lee HJ, Aschheim MA, Kuchma D. Interstory drift estimates for low-rise flexible diaphragm structures, *Engineering Structures*, **29**(2007) 1375-97.

10. Lee HJ, Kuchma D, Aschheim MA. Strength-based design of flexible diaphragms in low-rise structures subjected to earthquake loading, *Engineering Structures*, **29**(2007) 1277-95.
11. Khalili Jahromi K, Zahrai SM, Sarkissian L, Moslehitabar A, Koosha F. *Experimental and Analytical Case Study of Diaphragm Performance in Composite Slabs under Lateral Load*, BHRC Publication, No. R-483, 2008.
12. Sadashiva VK, MacRae GA, Deam BL, Spooner MS. Quantifying the seismic response of structures with flexible diaphragms, *Earthquake Engineering & Structural Dynamics*, No. 10, **41**(2012) 1365-89.
13. Hadianfard MA, Sedaghat S. Investigation of joist floor diaphragm flexibility on inelastic behavior of steel braced structures, *Scientia Iranica*, DOI: 10.1016/j.scient.2012.11.016, No. 3, **20**(2013) 445-53.
14. Abeysinghe CM, Thambiratnam DP, Perera NJ. Dynamic performance characteristics of an innovative Hybrid Composite Floor Plate System under human-induced loads, *Composite Structures*, **96**(2013) 590-600.
15. da Silva JGS, de Andrade SAL, Lopes EDC. Parametric modeling of the dynamic behavior of a steel–concrete composite floor, *Engineering Structures*, **75**(2014) 327-39.
16. Ministry of Housing and Urban Development, Iranian National Building Code, Part 6: Loads, 2013.
17. American Institute of Steel Construction, AISC Seismic provisions for structural steel buildings, Chicago, IL, 2010.
18. Viest IM, Colaco JP, Furlong RW, Griffs LG, Leon RT, Wyllie LA, *Composite Construction Design for Buildings*, Mc Graw-Hill, 1996.
19. BHRC. Iranian code of practice for seismic resistant design of buildings, Standard No. 2800, Tehran, Iran, 2014.
20. Sarkissian L. Study of the behavior of the composite floor systems under lateral load, M.Sc. Thesis, University of Tehran, 2005.
21. Sarkissian L, Khalili Jahromi K, Zahrai SM. Impact of joists direction on the diaphragm behavior of composite floor systems, *Journal of Seismology and Earthquake Engineering***,** No.1, **8**(2006) 29-38.
22. ANSYS (Revision 5.4). User's Manual, Theory, Swanson Analysis Systems Inc, **IV**(1997).